



## Mesoporous SBA-15 modified with manganese pyrazolylpyridine complexes for the catalytic epoxidation of terminal alkenes

Jianyuan Tang<sup>a</sup>, Yanhong Zu<sup>a</sup>, Weitao Huo<sup>a</sup>, Lei Wang<sup>a,b</sup>, Jing Wang<sup>a</sup>, Mingjun Jia<sup>a,\*</sup>, Wenxiang Zhang<sup>a</sup>, Werner R. Thiel<sup>b,\*\*</sup>

<sup>a</sup> State Key Laboratory of Theoretical and Computational Chemistry, College of Chemistry, Jilin University, 130021 Changchun, China

<sup>b</sup> Technische Universität Kaiserslautern, Fachbereich Chemie, Erwin-Schrödinger-Str., Geb. 54, Kaiserslautern 67663, Germany

### ARTICLE INFO

#### Article history:

Received 30 September 2011

Received in revised form

11 December 2011

Accepted 12 December 2011

Available online 21 December 2011

#### Keywords:

Epoxidation

Hybrid materials

Manganese acetate

Pyrazolylpyridine

### ABSTRACT

A manganese-based hybrid mesoporous material (denoted as **5**) was synthesized by covalent grafting of  $[\text{Mn}^{\text{II}}(\mathbf{1})_2](\text{OAc})_2$  (**3**) ( $\mathbf{1} = [3-(2\text{-pyridyl})\text{pyrazol-1-yl}]\text{acetic acid amide}$ ) onto the surface of SBA-15, and characterized by means of XRD,  $\text{N}_2$  adsorption-desorption, FT-IR, Raman, EPR and UV-vis spectroscopic techniques. Catalytic tests showed that **5** could act as an efficient heterogeneous catalyst for the epoxidation of a wide range of alkenes (including terminal ones) under mild reaction conditions when peracids (e.g., *meta*-chloroperbenzoic acid) are used as oxidants. Moreover, the catalytic performance of **5** is solvent-dependent, it exhibits higher catalytic activity and selectivity to epoxides when the reaction is carried out in aprotic solvent like  $\text{CH}_3\text{CN}$ . UV-vis and electrochemical measurements revealed that high-valent Mn species are easily formed during the reaction course, when *meta*-chloroperbenzoic acid is used as oxidant and  $\text{CH}_3\text{CN}$  is used as solvent, being probably the main reason for the high activity of **5** and its selectivity toward epoxide formation.

© 2011 Elsevier B.V. All rights reserved.

### 1. Introduction

Epoxidation of alkenes is an important reaction since the epoxides are key building blocks for the synthesis of fine chemicals and modern industrial processes [1,2]. Particularly, terminal alkenes are a challenging class of substrates to epoxidize owing to their relatively electron-deficient nature [3,4]. By using oxidants such as peracids, some electron-deficient and aliphatic terminal alkenes can be epoxidized even without adding catalysts. However, relatively high reaction temperatures (normally accompanied with low epoxide selectivity) and extended reaction times are usually required in this uncatalyzed process [5–7]. These drawbacks might be overcome if a suitable catalyst is adopted into the reaction system [8–12]. It was reported that Mn-containing complexes are active homogeneous catalysts for the epoxidation of terminal alkenes with peracids as the oxidants. For example, Kim et al. reported that a catalyst, which is composed of  $[\text{Re}_4\text{Q}_4(\text{CN})_{12}]^{4-}$  cluster anions (Q = Se or Te) surrounded by saloph-Mn<sup>III</sup> (saloph = N,N'-o-phenylenebis-salicylideneaminato) complexes through bridging CN ligands, exhibits very high activity for the epoxidation of various alkenes (including terminal alkenes)

using *meta*-chloroperbenzoic acid (m-CPBA) as oxidant at room temperature [13]. Stack et al. described a highly active homogeneous epoxidation catalyst system with peracetic acids as oxidants based on in situ prepared mononuclear manganese (II) complexes by mixing  $\text{Mn}(\text{CF}_3\text{SO}_3)_2$  and aromatic bidentate nitrogen ligands like 2,2'-bipyridyl or 1,10-phenanthroline [14,15].

Recently, more work has been focused on the heterogenization of homogeneous Mn-complexes catalysts, since such heterogeneous systems are more environmentally benign with respect to waste production and catalyst separation and recovery [16–20]. Moghadam et al. reported that Mn(porphyrin)Cl and Mn(saloph)Cl complexes covalently grafted on multi-wall carbon nanotubes showed moderate activity in the epoxidation of terminal olefins when  $\text{NaIO}_4$  was used as oxidant [21,22]. Assis et al. designed a polymer-supported catalyst by immobilizing Mn(salen)Cl onto chitosan membrane, and found that this catalyst was active for the epoxidation of cyclooctene and styrene with m-CPBA, although obvious decrease in activity was observed after recovery [23]. In another work reported by Stack et al.,  $[\text{Mn}^{\text{II}}(\text{phen})_2](\text{CF}_3\text{SO}_3)_2$  was immobilized onto mesoporous SBA-15 via a metal-template/metal-exchange route [24]. This material could be used as efficient and recyclable heterogeneous epoxidation catalyst with peracetic acid as the oxidant, and exhibited a greater substrate scope, a more efficient use of oxidant, and a higher reactivity than its homogeneous analogues. In spite of these considerable progresses, it is still an interesting and significant subject to develop novel heterogeneous

\* Corresponding author. Tel.: +86 431 85155390; fax: +86 431 88499140.

\*\* Corresponding author. Tel.: +49 631 2052752; fax: +49 631 2054676.

E-mail addresses: [jjamj@jlu.edu.cn](mailto:jjamj@jlu.edu.cn) (M. Jia), [thiel@chemie.uni-kl.de](mailto:thiel@chemie.uni-kl.de) (W.R. Thiel).

systems based on inexpensive and non-toxic metal catalysts, allowing an efficient epoxidation of electron-deficient alkenes under mild conditions.

Our previous work suggested that pyrazolopyridine ligands have special coordination ability allowing to generate active and stable Mo- or W-based heterogeneous epoxidation catalysts with *t*-BuOOH or H<sub>2</sub>O<sub>2</sub> as the oxidant [25–27]. In this work, SBA-15 supported manganese complexes of the type [Mn<sup>II</sup>(**1**)<sub>2</sub>](OAc)<sub>2</sub> (**1** = pyrazolopyridine ligand) are prepared by a post grafting method. Their catalytic properties for the epoxidation of alkenes (mainly for terminal alkenes) with peracids as oxidants are investigated. Furthermore, the influence of different reaction parameters – such as the oxidants and solvents – on the catalytic performance of the grafted Mn-complexes has been studied and will be discussed.

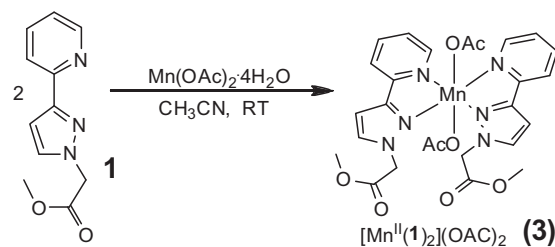
## 2. Experimental

### 2.1. Materials

Triblock copolymer EO<sub>20</sub>–PO<sub>70</sub>–EO<sub>20</sub> (P-123) (Aldrich), tetraethylorthosilicate (TEOS, Aldrich), Mn(OAc)<sub>2</sub>·4H<sub>2</sub>O (Acros), (3-aminopropyl)triethoxysilane (Sigma–Aldrich), *meta*-chloroperbenzoic acid (*m*-CPBA, Acros), *n*-dodecane (Merck), anhydrous acetonitrile (MeCN) (Aldrich), 1-octene (Acros), cyclooctene (Acros), styrene (Alfa Aesar), *a*-methylstyrene (Alfa Aesar), *trans*-stilbene (Alfa Aesar), were used as received without any further pretreatment. Other commercially available chemicals were laboratory-grade reagents from local suppliers.

### 2.2. Characterization methods

Powder XRD diffraction patterns were recorded on a Shimadzu XRD-6000 diffractometer (40 kV, 30 mA) using Ni-filtered Cu K $\alpha$  radiation. Microanalyses (C,H,N) were performed with a Perkin-Elmer 2400. N<sub>2</sub> adsorption/desorption isotherms were measured at –196 °C using a Micromeritics ASAP 2010N analyzer. Samples were degassed at 150 °C for 8 h before measurements. Specific surface areas were calculated using the BET model. Pore volumes are estimated at a relative pressure of 0.94 (*P/P*<sub>0</sub>), assuming full surface saturation with nitrogen. Pore size distributions are evaluated from desorption branches of the nitrogen isotherms using the BJH model. FT-IR spectra (KBr pellets) were recorded using a Nicolet Impact 410 spectrometer. Raman spectra were recorded on a Bruker RFS100/S FT instrument (Nd:YAG laser, 1064 nm excitation, InGaAs detector). EPR spectra were recorded with a JEOL JES-FA200 at X-band frequency ( $\nu \approx 9.44$  GHz, microwave power 1 mW, modulation frequency 100 kHz). The UV–vis spectra were recorded on a Shimadzu 3600 instrument. The solution of samples in CH<sub>3</sub>CN (or CH<sub>3</sub>CH<sub>2</sub>OH) was poured into a 1 cm quartz cell for UV–vis adsorption with CH<sub>3</sub>CN (or CH<sub>3</sub>CH<sub>2</sub>OH) as the reference. UV–vis spectra of the solid samples were recorded in the spectrophotometer with an integrating sphere using BaSO<sub>4</sub> as the standard. Electrochemical measurements were performed with a CHI660B electrochemical station in a conventional three-electrode cell under nitrogen atmosphere at room temperature. In CH<sub>3</sub>CN medium, the electrolyte was 0.1 M Bu<sub>4</sub>NClO<sub>4</sub> and potentials were referred to an Ag/10 mM AgNO<sub>3</sub> reference electrode in CH<sub>3</sub>CN, 0.1 M Bu<sub>4</sub>NClO<sub>4</sub> electrolyte. Potentials referred to that system can be converted to the ferrocene/ferricinium couple by subtracting 87 mV. The working electrode was a platinum disk (5 mm in diameter) polished with 2  $\mu$ m diamond paste (Mecaprex Presi) for cyclic voltammetry. Inductively Coupled Plasma Atomic Emission Spectroscopy (ICP-AES) analyses were conducted on a Perkin Elmer emission spectrometer. Each 10–20 mg sample of vacuum-dried material was dissolved in 1 mL of boiling 5% KOH solution and then



**Scheme 1.** Synthesis of [Mn<sup>II</sup>(**1**)<sub>2</sub>](OAc)<sub>2</sub> (**3**).

diluted to 10 mL with deionized water. A 5 mL aliquot was acidified with 1 mL of concentrated HNO<sub>3</sub> before diluted to 10 mL with deionized water. Each solution was filtered through a polyethersulfone filter and then submitted for metal analysis [24].

### 2.3. Preparation of catalysts

#### 2.3.1. Synthesis of ligands

[3-(2-Pyridyl)pyrazol-1-yl]acetic acid methylester (**1**) and (3-triethoxysilylpropyl)[3-(2-pyridylpyrazol)-1-yl]acetamide (**2**) were prepared according to procedures published in the literature [25,28].

#### 2.3.2. Preparation of complex [Mn<sup>II</sup>(**1**)<sub>2</sub>](OAc)<sub>2</sub> (**3**)

Mn(OAc)<sub>2</sub>·4H<sub>2</sub>O (0.7 mmol) and ligand (**1**) (1.4 mmol) were dissolved in dry CH<sub>3</sub>CN (25 mL). The mixture was stirred at room temperature for 4 h. The solvent was evaporated under vacuum in a rotary evaporator at a bath temperature of 65 °C resulting in a brown solid, which was washed with cold diethyl ether and dried at 80 °C (see Scheme 1). Elemental analysis for complex **3** Found: C, 50.8; H, 4.71; N, 13.6; Mn, 9.2%. Calcd.: C, 51.4; H, 4.6; N, 13.8; Mn, 9.1%. FT-IR (KBr, cm<sup>-1</sup>, selected peaks): 2857, 2922, and 2963:  $\nu$ (CH<sub>2</sub>); 1750:  $\nu$ (C=O); 1632:  $\nu$ (C=N), 545:  $\nu$ (Mn–N).

#### 2.3.3. Preparation of the mesoporous SBA-15 Materials

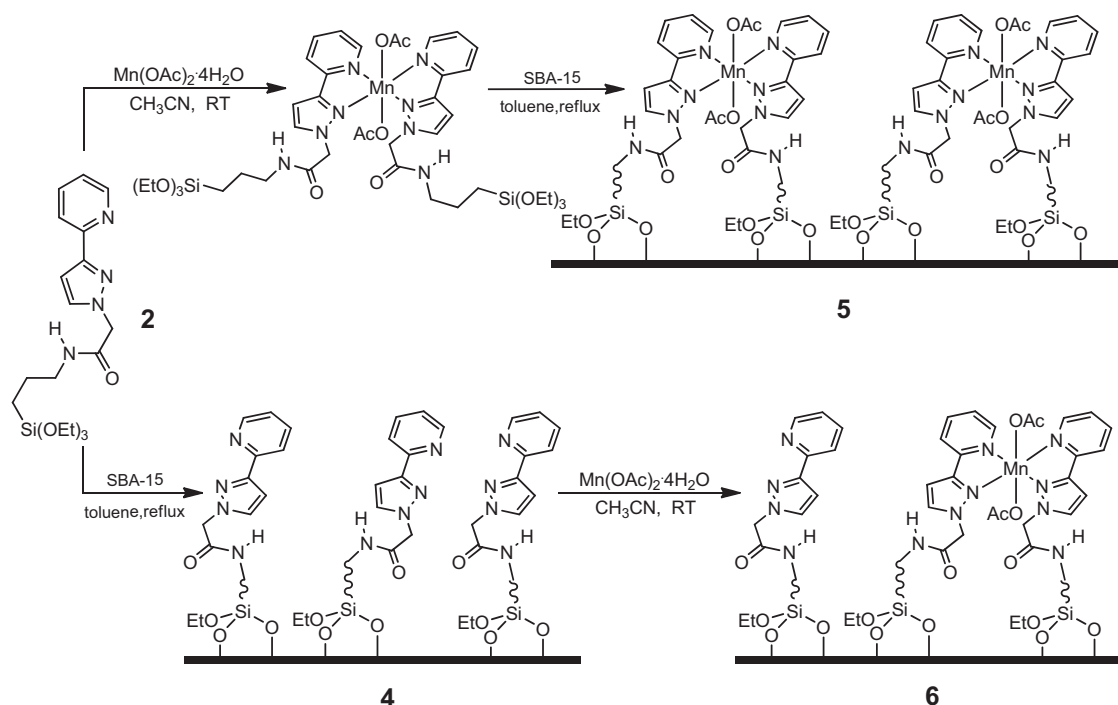
Mesoporous SBA-15 was prepared according to the literature using a triblock copolymer as the surfactant template [29]. In a typical synthesis, the triblock copolymer (P-123) (8.0 g) was dissolved in distilled water (60 mL) and 2 M HCl (240 mL) with stirring at 40 °C. Once the solution was visibly homogeneous, TEOS (18 mL) were added into that solution with stirring at 40 °C for 6 h. The mixture was aged at 100 °C for 48 h without stirring. The resulting material was filtered, washed with deionized water and ethanol, air-dried, and finally calcined, first at 350 °C for 2 h and then at 550 °C for 6 h to remove the template.

#### 2.3.4. Preparation of the hybrid material **5**

Mn(OAc)<sub>2</sub>·4H<sub>2</sub>O (0.15 mmol) and (3-triethoxysilylpropyl)[3-(2-pyridyl)pyrazol-1-yl]acetamide (**2**) (0.30 mmol) were dissolved in dry CH<sub>3</sub>CN (25 mL) in a 150 mL Schlenk flask under N<sub>2</sub>. The solution was stirred at room temperature for 12 h to form a brown solution. Approximately 40 mL of toluene were added before the addition of SBA-15 (1.0 g) (pre-activated by heating to 160 °C under vacuum for 3 h). The mixture was heated to reflux for 24 h under N<sub>2</sub>. The resulting solid (denoted as **5**) was filtered, washed, Soxhlet-extracted with chloroform for 24 h, and dried in the vacuum at 70 °C (see Scheme 2).

#### 2.3.5. Preparation of reference sample **6**

The mesoporous support SBA-15 (1.0 g), was first pre-activated by heating to 160 °C under vacuum for 3 h. After cooling and release of the vacuum, **2** (0.21 mmol in 40 mL of toluene) was added under a N<sub>2</sub> atmosphere and the mixture was heated to reflux for 24 h.



**Scheme 2.** Preparation of hybrid mesoporous materials **5** and **6**.

The resulting solid (denoted as **4**) was filtered, washed, Soxhlet-extracted with chloroform for 24 h, and dried in the vacuum at 70 °C. After that, hybrid material **4** (1.0 g) was stirred with 0.040 g  $\text{Mn}(\text{OAc})_2 \cdot 4\text{H}_2\text{O}$  (dissolved in 60 mL of  $\text{CHCl}_3$ ) at room temperature for 24 h. The resulting sample **6** was filtered off, Soxhlet-extracted with  $\text{CHCl}_3$  to remove untethered species and dried in vacuum (see [Scheme 2](#)). The composition of the grafted samples **5** and **6** is summarized in [Table 1](#).

#### 2.4. Representative epoxidation conditions

Epoxidation of alkenes was typically performed according to the following procedure: substrate (0.5 mmol), the heterogeneous catalyst (25 mg, equiv. to 0.0035 mmol of Mn, 0.7 mol% relative to the alkene) suspended in the solvent (2 mL), and *n*-dodecane (0.5 mmol, internal standard) were combined in a 10-mL glass flask with a stir bar. The mixture was pre-cooled to the indicated temperature, and then oxidant (1.0 mmol, e.g., *m*-CPBA) was added in four roughly equal portions over a 2 min period, the mixture was stirred for an additional 28 min. Gas chromatography was employed to monitor the progress of the epoxidation reaction. After completion of the reaction, the catalyst was removed by filtration, washed with acetone, and dried in air. The remaining catalyst used in subsequent trials was assumed to fully retain all of the initial manganese. Isolated epoxides: The epoxide product was extracted into pentane (3 mL  $\times$  4 mL), washed with 1 M  $\text{NaHCO}_3$  (aq) and dried over sodium sulfate. The organic solvent was removed under vacuum by rotary

evaporator. The crude product was purified by a silica gel column with dichloromethane as the eluent to give the desired epoxides as a colorless liquid. The epoxides were characterized by GC–MS or  $^1\text{H}$  NMR spectrum, and compared with the known compounds.

### 3. Results and discussion

#### 3.1. Catalyst Characterization

The FT-IR spectra of **SBA-15**, complex **3**, the hybrid materials **5** and **6** are shown in [Fig. 1](#). In the 2800–4000  $\text{cm}^{-1}$  region, the sharp band at 3740  $\text{cm}^{-1}$  in the spectrum of the SBA-15 support is assigned to free surface Si–OH groups ([Fig. 1b](#)). For the hybrid materials **5** and **6**, the relative intensities of these Si–OH vibrations obviously decrease compared with the neat SBA-15, indicating that the condensation reaction to form Si–O–Si bonds between the organosilane moieties and the surface Si–OH groups of SBA-15 has occurred under our experimental conditions [[27](#)]. The bands at 2857, 2922, and 2963  $\text{cm}^{-1}$ , being absent in the spectrum of the neat support but present in the spectra of the hybrid materials **5** and **6**, are attributed to  $\nu(\text{CH}_2)$  of the propyl arm of the ligand.

In the region of 1250–1800  $\text{cm}^{-1}$ , SBA-15 support exhibited a broad band at around 1635  $\text{cm}^{-1}$  due to the  $\nu(\text{O–H})$  of adsorbed water. The C=N groups in the hybrid materials, should give a characteristic band overlapped by this O–H bending vibration band [[30](#)]. The bands centered at around 1635  $\text{cm}^{-1}$  in the spectra of the hybrid materials shifted slightly to higher wavenumbers and increased in intensity. Moreover, some additional weak peaks, appearing at 1550, 1437, 1403 and 1360  $\text{cm}^{-1}$ , are due to the presence of the organic ligands in the hybrid materials. Compared with the complex **3**, hybrid materials **5** and **6** show less and weaker bands related to the complex. The relatively low resolution for the introduced complex in the hybrid materials should be due to the strong IR absorbance of the siliceous base materials in a similar region.

Raman spectroscopy characterization has also been carried out on **5** and **6**. However, the resolution of the Raman spectra is very poor owing to the relatively low loading of ligand and complex in

**Table 1**

Characteristics of support and catalysts, specific surface area,  $S_{\text{BET}}$  ( $\text{m}^2 \text{g}^{-1}$ ); pore volume  $V_{\text{BjH}}$  ( $\text{cm}^3 \text{g}^{-1}$ ); pore diameter  $D_{\text{BjH}}$  (nm) the C, H, N analyses of the hybrid materials; C(Mn), initial concentration of Mn species ( $\text{mmol g}^{-1}$ ).

Entry	Materials	$S_{\text{BET}}$	$V_{\text{BjH}}$	$D_{\text{BjH}}$	Ligand <b>1</b> ( $\text{mmol g}^{-1}$ )	C(Mn) ( $\text{mmol g}^{-1}$ )
1	SBA-15	1160	1.72	6.8	–	–
2	<b>5</b>	629	1.04	6.4	0.28	0.14
3	<b>6</b>	702	1.16	6.3	0.20	0.14

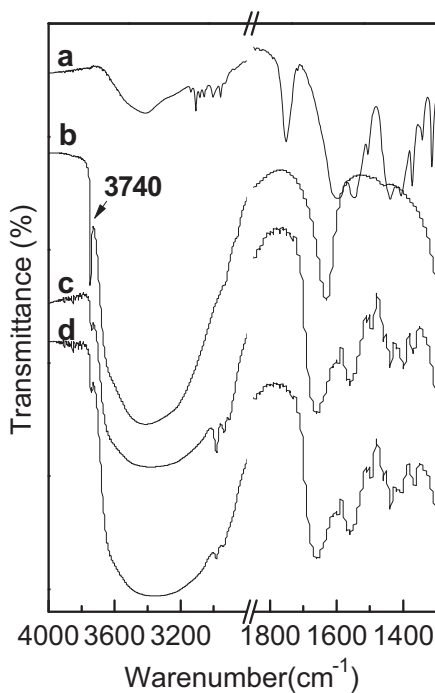


Fig. 1. FT-IR spectra of complex **3** (a); SBA-15 (b); **5** (c) and **6** (d).

the hybrid materials. The complexation of ligand with Mn species can be confirmed by comparing the Raman spectra of ligand **1** and complex **3** (Fig. 2), in which significant changes can be observed in the region between 1630 and 1430  $\text{cm}^{-1}$  in the bands assigned to ring skeletal stretching modes of the ligand N–C–C–N fragment [31–33].

The powder XRD patterns of the hybrid materials **5**, **6** and of neat SBA-15 are shown in Fig. 3. The SBA-15 sample shows three peaks, indexed as the (1 0 0), (1 1 0) and (2 0 0) diffraction peaks associated with typical two-dimensional hexagonal symmetry of the SBA-15 material (Fig. 3a) [29].

For the hybrid materials **5** and **6** the relative intensities of the prominent diffraction peak (1 0 0) decreased somewhat after introducing the chelate ligand and the manganese complex. However, the main reflections of the XRD pattern can still be observed. According to the related references [29,34], the intensity reduction may be mainly due to contrast matching between the silicate

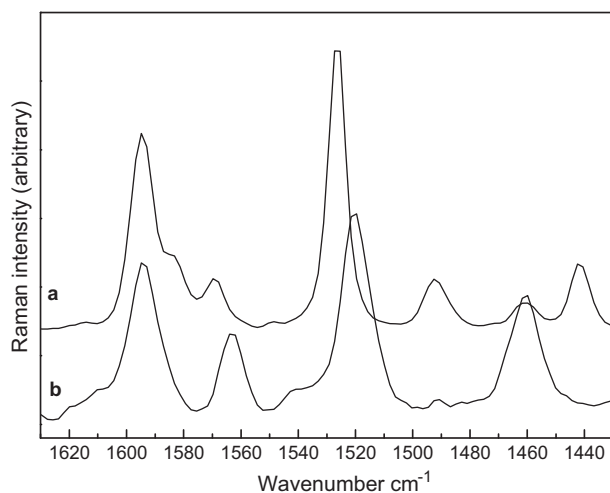


Fig. 2. Selected region of the Raman spectra of the free ligand **1** (a) and the corresponding manganese complex **3** (b).

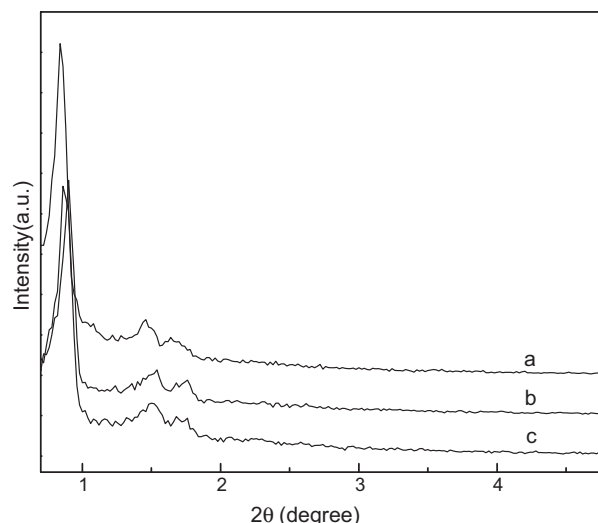


Fig. 3. Powder XRD patterns of SBA-15 (a); **5** (b) and **6** (c).

framework and organic moieties which are located inside the channels of SBA-15.

The  $\text{N}_2$  adsorption/desorption isotherms of the hybrid materials **5**, **6** and SBA-15 are shown in Fig. 4. Obviously, the hybrid materials **5** and **6** maintain the characteristics of type IV isotherms and show a uniform pore size distribution in the mesoporous region. Compared to SBA-15, a pronounced decrease in BET surface area, pore volume, and pore size of the hybrid materials occurs. This should be mainly caused by the introduction of ligand and/or the manganese complexes (Table 1). It should be mentioned here that, the ratio of ligand/Mn ratio in **6** is less than 2:1, which is slight lower than that of **5** (2:1). In this case, a considerable amount of mono-ligand coordinated Mn-complexes should be present in **6**, while bis-ligand coordinated Mn-complexes are dominant in **5**, as showed in Scheme 2.

### 3.2. Catalysis

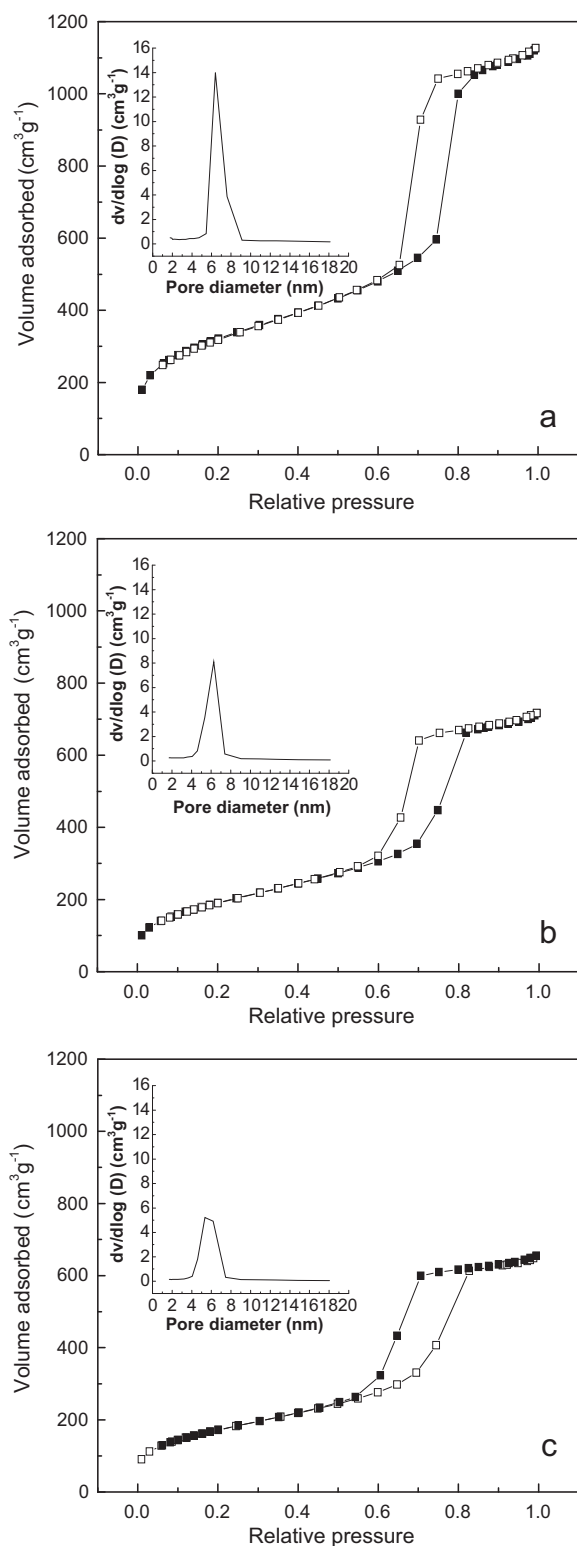
The catalytic properties of **5** and **6** in the epoxidation of styrene are shown in Table 2. For comparison, the reaction results of the homogeneous manganese(II) acetate complex  $[\text{Mn}^{\text{II}}(\mathbf{1})_2](\text{OAc})_2$  (**3**) are also given. When *m*-CPBA was used as oxidant in combination with  $\text{CH}_3\text{CN}$  as solvent, all catalysts were active for the epoxidation of styrene. The complex **3** was found to be the most active catalyst for epoxidation of styrene with a TOF of  $841 \text{ h}^{-1}$ , which was much higher than that of homogeneous manganese(II) acetate ( $\text{TOF } 531 \text{ h}^{-1}$ ). The hybrid catalysts **5** and **6** were also quite active, with TOFs of 583 and  $612 \text{ h}^{-1}$ , respectively. Besides, **5** showed very high selectivity to styrene epoxide, and a 96% selectivity of styrene

Table 2  
Epoxidation reactivity of various catalysts with styrene.<sup>a</sup>

Entry	Catalysts	Conv. (%)	TOF ( $\text{h}^{-1}$ )	Product sel. (%) <sup>b</sup>		
				SO	BA	PA
1	$\text{Mn}(\text{OAc})_2 \cdot 4\text{H}_2\text{O}$	90	531	83	13	4
2	<b>3</b>	>99	841	93	5	2
3	<b>5</b>	>99	612	96	3	1
4	<b>6</b>	95	583	94	5	1

<sup>a</sup> Reaction conditions: 0.5 mmol of olefin, 1.0 mmol of *m*-CPBA, 0.5 mmol of *n*-dodecane (internal standard), 0.7 mmol% of Mn, and 2 mL of  $\text{CH}_3\text{CN}$ ; reaction temperature  $0^\circ\text{C}$ ; reaction time (30 min); TOF, average turnover frequency in the first 10 min per active site.

<sup>b</sup> SO, styrene oxide; BA, benzaldehyde; PA, phenylacetaldehyde.



**Fig. 4.** N<sub>2</sub> adsorption/desorption isotherms at 77 K and pore size distribution profiles (inset) of SBA-15 (a); **5** (b) and **6** (c).

epoxide (with >99% conversion of styrene) could be achieved after 30 min reaction.

The catalytic activity of **5** was further studied in the epoxidation of styrene using different oxidants, including NaClO, NaIO<sub>4</sub>, *t*-BuOOH and H<sub>2</sub>O<sub>2</sub> (30%). When *t*-BuOOH, NaClO and NaIO<sub>4</sub> were used as oxidants, **5** also showed high activity for the epoxidation of styrene at room temperature. However, large amounts of

**Table 3**  
Effect of oxidant on the epoxidation of styrene catalyzed by **5**.<sup>a</sup>

Entry	Oxidant	T (°C)	t (h)	Conv. (%)	TOF (h <sup>-1</sup> )	Product sel. (%) <sup>b</sup>		
						SO	BA	PA
1	<i>m</i> -CPBA	0	0.5	>99	612	96	3	1
2	<i>m</i> -CPBA	25	0.5	>99	771	91	6	3
3	<i>tert</i> -BuOOH	25	48	95	5 <sup>c</sup>	22	78	n.d.
4	NaClO <sup>d</sup>	25	12	99	16 <sup>c</sup>	52	42	6
5	NaIO <sub>4</sub> <sup>e</sup>	25	24	92	8 <sup>c</sup>	65	32	5
6	H <sub>2</sub> O <sub>2</sub>	25	24	n.d.	n.d.	n.d.	n.d.	n.d.
7	H <sub>2</sub> O <sub>2</sub> <sup>f</sup>	25	24	96	10 <sup>c</sup>	96	1	2

<sup>a</sup> Reaction conditions: olefin (0.5 mmol), oxidant (1.0 mmol), *n*-dodecane (internal standard, 0.5 mmol), catalyst (0.7 mmol% of Mn, 25 mg), and CH<sub>3</sub>CN (2 mL); TOF, average turnover frequency in first 10 min per active site.

<sup>b</sup> SO, styrene oxide; BA, benzaldehyde; PA, phenylacetaldehyde.

<sup>c</sup> TOF, average turnover frequency in first hour per active site.

<sup>d</sup> NaClO (pH 11.5, 0.55 M) [30].

<sup>e</sup> NaIO<sub>4</sub> [21,22].

<sup>f</sup> H<sub>2</sub>O<sub>2</sub> (1.0 mmol); imidazole (0.07 mmol), NaHCO<sub>3</sub> (0.5 mmol) [36].

by-products (benzaldehyde and phenylacetaldehyde) were produced in these systems. Similar results have been reported for Mn(porphyrin)- and Mn(salen)-based heterogeneous epoxidation catalysts [21–23]. When H<sub>2</sub>O<sub>2</sub> (30%) was used as the oxygen source, no detectable conversion of styrene could be observed after 24 h reaction. This might be due to the fact that **5** possess a strong ability for the decomposition of H<sub>2</sub>O<sub>2</sub> to water and oxygen [35]. Notably, the rapid decomposition of hydrogen peroxide could be effectively inhibited over catalyst **5** when some additives like imidazole and NaHCO<sub>3</sub> were introduced into the reaction system, thus very high styrene conversion and epoxide selectivity could be achieved under the same reaction conditions (Table 3, entry 6). It should be mentioned here that the selectivity of epoxide decrease somewhat (from 96% to 91%) with *m*-CPBA as the oxidant when the reaction temperature increases from 0 °C to 25 °C (Table 3, entry 2).

The effect of various solvents on the epoxidation of styrene was also investigated for catalyst **5**. Table 4 summarizes the results of a comparative study on the epoxidation of styrene with the catalyst of **5** and *m*-CPBA in protic (CH<sub>3</sub>OH and C<sub>2</sub>H<sub>5</sub>OH) and aprotic solvents (CH<sub>3</sub>COOC<sub>2</sub>H<sub>5</sub>, CH<sub>2</sub>Cl<sub>2</sub> and CH<sub>3</sub>CN). As expected, the catalytic activity was related to the solvent. It is found that the conversion of styrene was much higher in aprotic than in protic solvents (Table 4).

The catalytic properties of **5** and **6** were explored for the epoxidation of different alkenes using *m*-CPBA as oxidant at 0 °C (Table 5). For the catalyst **5**, cyclooctene was oxidized with >99% of conversion and >99% selectivity to the epoxide after 10 min (TOF 856 h<sup>-1</sup>). Oxidation of *a*-methylstyrene produced 78% of *a*-methylstyrene epoxide and 22% of acetophenone at the similar reaction conditions. Moreover, the terminal alkene 1-octene was also readily epoxidized with *m*-CPBA as the oxidant and **5** as the catalyst: 91% of conversion with >99% selectivity to epoxide and 87% isolated yield could be obtained at 0 °C after 30 min reaction time (entry 7). Besides, *trans*-stilbene could be epoxidized in a stereospecific manner with

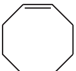
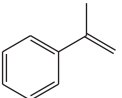
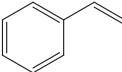
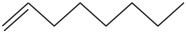
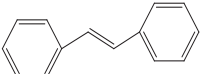
**Table 4**  
Effect of solvent on the epoxidation of styrene catalyzed by **5** at 0 °C.<sup>a</sup>

Entry	Solvent	Conv. (%)	TOF (h <sup>-1</sup> )	Product sel. (%) <sup>b</sup>		
				SO	BA	PA
1	CH <sub>3</sub> OH	49	284	93	4	3
2	C <sub>2</sub> H <sub>5</sub> OH	34	257	94	4	2
3	CH <sub>3</sub> COOC <sub>2</sub> H <sub>5</sub>	74	465	93	7	n.d.
4	CH <sub>2</sub> Cl <sub>2</sub>	91	573	94	5	1
5	CH <sub>3</sub> CN	>99	612	96	3	1

<sup>a</sup> Reaction conditions: styrene (0.5 mmol), *m*-CPBA (1.0 mmol), *n*-dodecane (internal standard, 0.5 mmol), **5** (0.7 mmol% Mn, 25 mg), and solvent (2 mL); reaction temperature (0 °C); TOF, turnover frequency in first 10 min per active site.

<sup>b</sup> SO, styrene oxide; BA, benzaldehyde; PA, phenylacetaldehyde.

**Table 5**  
Epoxidation of various olefins with *m*-CPBA catalyzed by **5** and **6**.<sup>a</sup>

Entry	Substrate	Catalysts	<i>t</i> (min)	Conv. (%)	TOF (h <sup>-1</sup> )	Epoxide sel. (%)
1		5	10	>99	856	>99
2		6	10	>99	856	>99
3		5	10	>99	856	78
4		6	10	>99	856	71
5		5	30	>99	612	96
6		6	30	95	583	94
7		5	30	91	446	>99
8		6	30	80	427	>99
9		5	60	66	94 <sup>b</sup>	>99
10		6	60	54	77 <sup>b</sup>	>99

<sup>a</sup> Reaction conditions: olefin (0.5 mmol), *m*-CPBA (1.0 mmol), *n*-dodecane (internal standard, 0.5 mmol), the heterogeneous catalyst (0.7 mmol% of Mn, 25 mg), and CH<sub>3</sub>CN (2 mL); reaction temperature (0 °C); TOF, turnover frequency in first 10 min per active site.

<sup>b</sup> Turnover frequency in first hour per active site.

complete retention of configuration (66% conversion with >99% selectivity to the major product after 60 min, TOF 94 h<sup>-1</sup>). Compared with **5**, the catalytic activity and/or epoxide yield of catalyst **6** was usually lower under the same reaction conditions.

Fig. 5A shows the kinetic profiles of epoxidation of 1-octene with CH<sub>3</sub>CN as the solvent over **5** and **6**. In a duplicate reaction, the leaching test was also performed to verify the heterogeneity of the catalytic process (Fig. 5B). It should be mentioned firstly that a blank reaction (without adding any catalyst) using the mixed solvent gave a conversion of 1-octene of about 4.5% after a reaction time of 2 h. With **5** as the catalyst, the conversion of 1-octene reached 31% after 5 min. After removing the catalyst by filtration, the conversion of 1-octene increased to 36% during the following 115 min. In the case of **6** as the catalyst, the conversion of 1-octene increased from 28 to 47% after removing the catalyst. Taking the result of the blank reaction into account, it can be concluded here that **5** is truly heterogeneous catalyst under the test condition and no obvious leaching of active catalytic species occurs during the reaction. On the other hand, a small part of active Mn activates should be leached from the hybrid **6** catalyst during the reaction course.

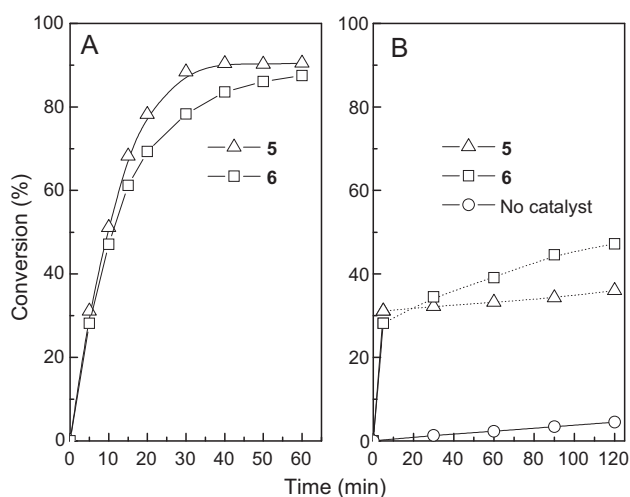


**Fig. 5.** (A) Kinetic profiles of the epoxidation of 1-octene with *m*-CPBA over **5** and **6** in the presence of CH<sub>3</sub>CN. (B) Leaching experiments of two Mn-containing catalysts (dashed lines indicate the conversions after the removal of the catalysts). Reaction conditions are analogous to Table 5.

The recycling experiments of **5** and **6** for the epoxidation of 1-octene were also carried out with *m*-CPBA as the oxidant and CH<sub>3</sub>CN as the solvent (Table 6). After each experiment, the filtered catalysts were washed with CH<sub>3</sub>CN and dried at 60 °C, then reused without further treatment. The catalyst **5** showed very good recyclability, no obvious change in activity could be observed with the increase of recyclable number, and the conversion of 1-octene still remains at around 90% after six reaction cycles (Table 6); while the catalyst **6** demonstrated a gradual decrease in activity with increasing the numbers of recycling experiments. The results of the ICP analysis provide a further evidence that Mn species in **5** were very stable during the reaction process, since the Mn content for the used catalyst of **5** (after the 6th reaction) just decreased slightly (from 0.14 mmol g<sup>-1</sup> to 0.13 mmol g<sup>-1</sup>) compared with the fresh one. As for **6**, an obvious decrease of the Mn content (from 0.14 mmol g<sup>-1</sup> to 0.10 mmol g<sup>-1</sup>) can be observed after the 6th reaction.

Our previous work has shown that pyrazolylpyridines are suitable to form active and stable Mo- and W-based epoxidation catalysts due to their special coordination abilities [26,27]. As mentioned above, the main difference between **5** and **6** is: bis-ligand coordinated Mn-complexes are dominant in **5**, while a considerable amount of mono-ligand coordinated Mn-complexes should be present in **6**. Hence, we may conclude here that the perfect catalytic features of **5** should be mainly assigned to the presence of a strong coordinative interaction between the chelate ligand and the Mn species.

To understand the nature of catalyst **5**, EPR and UV-vis measurements were carried out for fresh and used catalyst **5** (after

**Table 6**  
Recyclability of **5** and **6** in the epoxidation of 1-octene with *m*-CPBA oxidant.<sup>a</sup>

Run	<b>5</b>		<b>6</b>	
	C(Mn) (mmol g <sup>-1</sup> ) <sup>b</sup>	Conv. (%)	C(Mn) (mmol g <sup>-1</sup> ) <sup>b</sup>	Conv. (%)
0	0.14		0.14	
1		91		85
2		89		80
3		90		79
4		92		77
5		89		75
6	0.13	90	0.10	72

<sup>a</sup> Reaction conditions: olefin (2.0 mmol), *m*-CPBA (4.0 mmol), heterogeneous catalyst (0.7 mmol% of Mn, 100 mg), and CH<sub>3</sub>CN (8 mL); reaction temperature (0 °C).

<sup>b</sup> Determined by ICP-AES analysis.

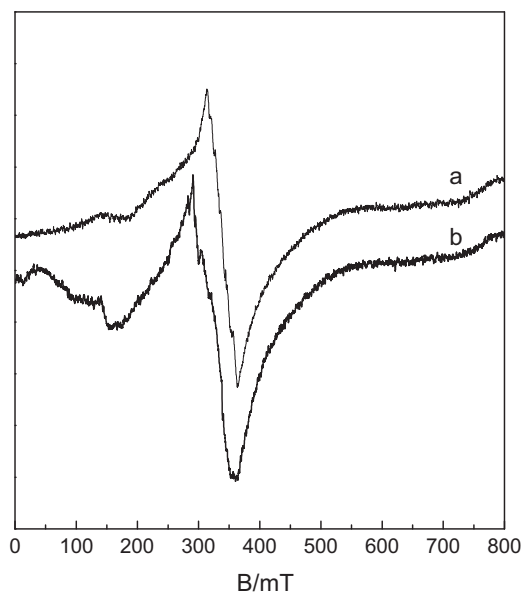


**Fig. 6.** EPR spectra of the fresh **5** (a) and the used **5** after the 6th reaction (b). Recording temperature:  $T = 20^\circ\text{C}$ .

the 6th reaction). EPR spectra of the two samples were recorded at room temperature using the conventional perpendicular detection mode (Fig. 6). Both spectra present features between 0 and 800 mT. The fresh **5** presents three main transitions at  $g_{\text{eff}} \approx 5.7$ , 2.9, and 2.0 (Fig. 6a).  $^{55}\text{Mn}$  hyperfine lines ( $I = 5/2$ ) are observed on the  $g_{\text{eff}} \approx 2.0$  transition and are separated by 8.5 mT, which is consistent with a high-spin ( $S = 5/2$ ) mononuclear Mn(II) species [37,38]. The appearance of a weak signal at lower field  $g_{\text{eff}} \approx 8.7$  in spectrum of used **5** implies the presence of a trace amount of high-valent Mn species. The diffuse reflectance UV–vis spectra of fresh and used **5** are given in Fig. 7. Strong bands at 248 and 285 nm can be attributed to the charge transfer transition of pyrazolylpyridine ligand (Fig. 7a). The appearance of weak and broad bands at about 330 and 400 nm in the spectrum of the used **5** should be also related to the presence of a small amount of high-valent Mn species [39], thus providing a further evidence that a part of Mn(II) species has been oxidized to a high-valent state by the oxidant during the reaction course.

Furthermore, electrochemical measurements were carried out to monitor the formation of reactive intermediates over the homogeneous complex  $\text{Mn}(\mathbf{1})_2(\text{OAc})_2(\mathbf{3})$  catalyst when different

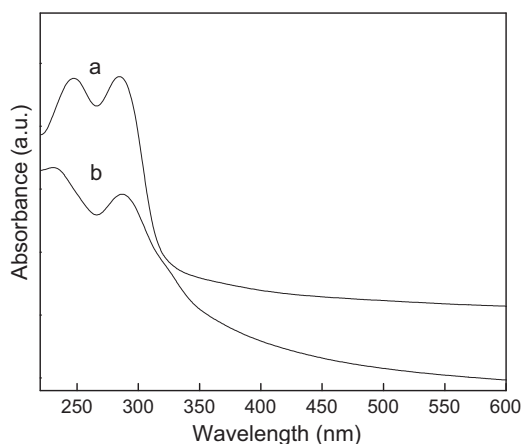


**Fig. 7.** The solid reflectance UV–vis spectra of fresh **5** (a) and used **5** after the 6th reaction (b).

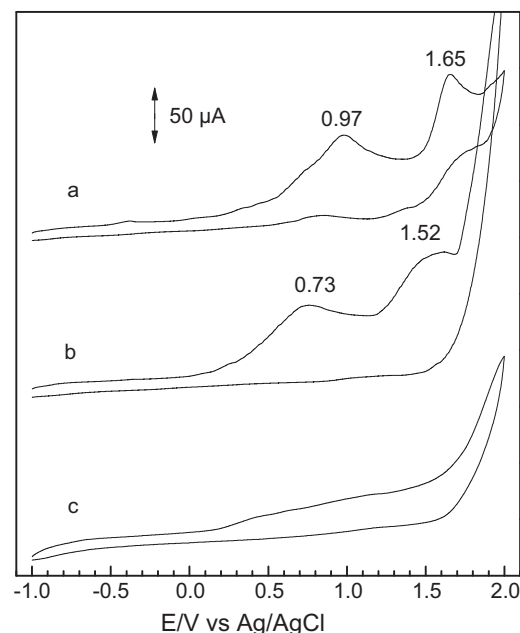


**Fig. 8.** (a) Cyclic voltammograms of a 1 mM acetonitrile solution of complex **3** in the presence of 0.1 M tetrabutylammonium perchlorate ( $T = 25^\circ\text{C}$ , scan rate  $100 \text{ mV s}^{-1}$ ); (b) after addition 2 equiv. of *t*-BuOOH per molecule of **3**; (c) after addition 2 equiv. of *m*-CPBA per molecule of **3**.

oxidants (i.e., *tert*-BuOOH and *m*-CPBA) are used for epoxidation reaction. The oxidation processes of the homogeneous complex **3** in acetonitrile at room temperature, measured by cyclic voltammetry (CV) are shown in Fig. 8a. For the CV of **3** in  $\text{CH}_3\text{CN}$ , two oxidation processes are detected, which located at  $E_{\text{pa}} = 0.90 \text{ V}$  and  $1.65 \text{ V}$  vs.  $\text{Ag}/\text{Ag}^+ 10^{-2} \text{ M}$ . The shape of the CV of **3** are quite similar to that of  $[(\text{L})\text{Mn}^{\text{II}}\text{Cl}(\text{OH}_2)]$  ( $\text{L} = \text{N}, \text{N}'\text{-dimethyl-N}, \text{N}'\text{-bis}(2\text{-pyridylmethyl})\text{propane-1,3-diamine}$ ) [37], and  $[\text{Mn}(\text{tolylterpy})_2]^{2+}$  [40]. Hence, the two oxidation waves can be assigned to the successive one-electron abstraction from Mn(II), leading to Mn(III), and from Mn(III), generating Mn(IV), respectively. The absence of reversibility of the two processes might be due to the potential high reactivity of the high valent manganese cation [41].

When two equiv. of *t*-BuOOH was added into the **3** solution, the two oxidation waves potential ( $E_{\text{pa}} = 0.90 \text{ V}$  and  $1.65 \text{ V}$  vs.  $\text{Ag}/\text{Ag}^+ 10^{-2} \text{ M}$ ) shift considerably toward lower positive potential located at  $0.7 \text{ V}$  and  $1.5 \text{ V}$  vs.  $\text{Ag}/\text{Ag}^+ 10^{-2} \text{ M}$  after 30 min (Fig. 8b). The observed changes in the cyclic voltammograms of the Mn-complex might be due to fact that the original anionic ligands of metal center have been replaced (at least partially) by *t*-BuOO $^-$ , and the higher donor capacity of the ligand *t*-BuOO $^-$  may result in an easy oxidation of the metal center (Mn cation) [42,43]. It should be mentioned that the solution color changed from light yellow to yellow in a few minutes after the addition of *t*-BuOOH, indicating that only a small amount of high-valent manganese species appeared in the solution.

Fig. 8c shows that the oxidation waves turn to very weak (nearly disappear) when two equiv. *m*-CPBA was added into acetonitrile solution of **3**. Besides, it was found that the solution color changed from light yellow to brown in a few minutes after the addition of *m*-CPBA. Hence, the change in the cyclic voltammograms might be due to the fact that a great number of high-valent Mn species have already appeared in the presence of *m*-CPBA oxidant (before electrochemical experiments).

UV–vis spectroscopy was also used to monitor the formation of reactive intermediates of the homogeneous catalyst **3** (dissolved in  $\text{CH}_3\text{CN}$  or  $\text{CH}_3\text{CH}_2\text{OH}$ ). First, a small amount of freshly prepared complex **3** was dissolved in  $\text{CH}_3\text{CN}$  (or  $\text{CH}_3\text{CH}_2\text{OH}$ ), then 20 equiv. of oxidant were added to the solution at room temperature. The

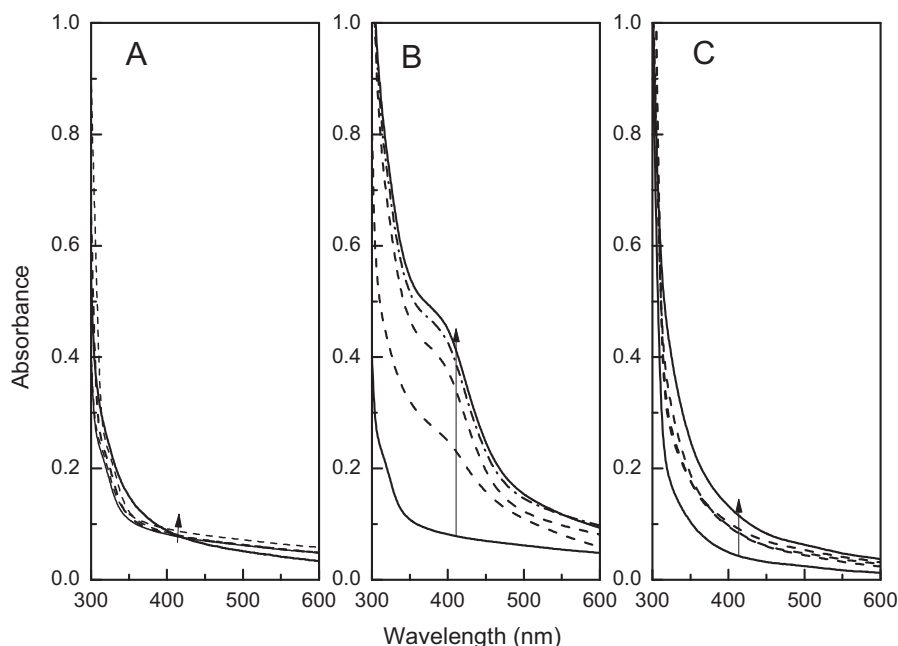


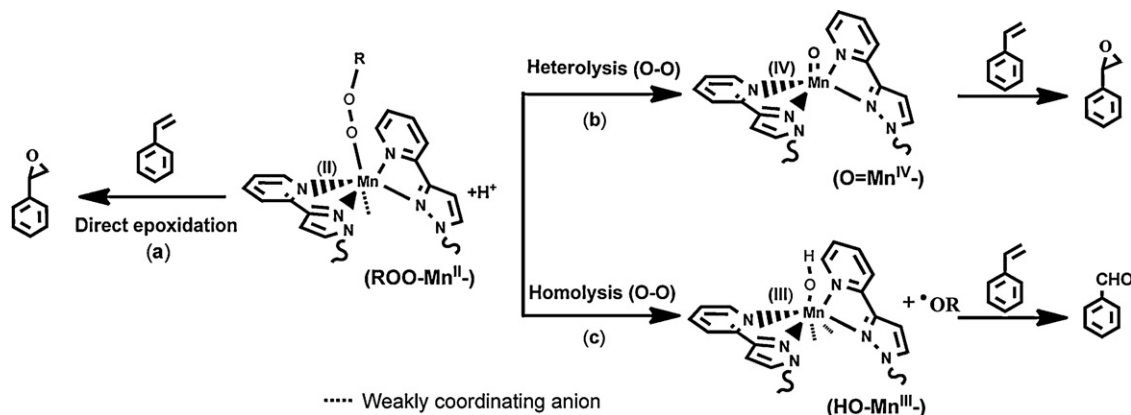
**Fig. 9.** UV-vis spectral changes during the reaction of complex **3** ( $4 \times 10^{-5}$  M) with 20 equiv. of oxidant in different solvents at room temperature. The spectra at 0, 5, 10, 20, 30 min after the addition of oxidant are shown. (A) oxidant: *t*-BuOOH, solvent:  $\text{CH}_3\text{CN}$ ; (B) oxidant: *m*-CPBA; solvent:  $\text{CH}_3\text{CN}$ ; (C) oxidant: *m*-CPBA; solvent:  $\text{CH}_3\text{CH}_2\text{OH}$ .

UV-vis spectra were recorded after the addition of the oxidant (see Fig. 9). When  $\text{CH}_3\text{CN}$  was used as the solvent, no obvious change could be observed after the addition of *t*-BuOOH for 30 min (Fig. 9A). It was supposed that the reactive intermediates might not be spectroscopically observable due to their low concentration and/or short lifetime. When *m*-CPBA was added into the **3** solution, it could be observed that the solution color changed from light yellow to brown in a few minutes, while an absorption band appeared at 410 nm, and its intensity grew rapidly with time (Fig. 9B). On the basis of related literatures [44,45] as well as the above electrochemical results, the appearance of 410 band might be mainly assigned to the formation of a great number of high-valent Mn species (e.g.,  $\text{O}=\text{Mn}^{\text{IV}}$ ) after the addition of *m*-CPBA. Besides, if aprotic solvent ( $\text{CH}_3\text{CN}$ ) was replaced by protic solvent ( $\text{CH}_3\text{CH}_2\text{OH}$ ), the absorption band at around 410 nm is nearly undetectable in the *m*-CPBA/ $\text{CH}_3\text{CH}_2\text{OH}$  system (Fig. 9C), this might be due to the fact that alcohol could act as a reducing solvent, which can easily react with the high valent manganese species upon its formation.

In previous reports [45–47], several groups have studied the reaction mechanism of the epoxidation in the presence of

Mn-containing catalysts, such as  $\text{Mn}^{\text{III}}(\text{salen})$ ,  $\text{Mn}^{\text{III}}(\text{porphyrin})$  and  $\text{Mn}^{\text{III}}(\text{nonheme})$ . It was reported that when a peroxidic oxygen donor such as  $\text{H}_2\text{O}_2$ , *t*-BuOOH or *m*-CPBA was used as the oxidant, an  $\text{ROO}-\text{Mn}^{\text{III}}$ -adduct was initially formed, which could epoxidize olefins directly by a Lewis acid mechanism. Besides, the O–O bond of the  $\text{ROO}-\text{Mn}^{\text{III}}$ -adduct may also be cleaved either heterolytically to form  $\text{O}=\text{Mn}^{\text{V}}$  species or homolytically to yield  $\text{HO}-\text{Mn}^{\text{IV}}$  species (actually the  $\text{HO}-\text{Mn}^{\text{IV}}$  radical cation). It was believed that the  $\text{O}=\text{Mn}^{\text{V}}$  species is an active intermediate and responsible for alkene epoxidation, whereas the  $\text{HO}-\text{Mn}^{\text{IV}}$  complex is invoked in radical-type oxidations to account for the formation of ring-opened or aldehyde products in the  $\text{Mn}^{\text{III}}(\text{salen})$  catalyzed epoxidation reactions [13,48].

On the basis of these reports and our results, we can say that the epoxidation of alkenes over catalyst **5** could also occur in different ways when different oxygen donors (oxidants) or solvents are used (Scheme 3). When *m*-CPBA was used as the oxidant for the epoxidation of styrene (with  $\text{CH}_3\text{CN}$  as the solvent), very high selectivity (ca. 96%) to epoxystyrene can be obtained with **5**, suggesting that pathway a or b should give significant contribution. When *t*-BuOOH was used as the oxidant, a large number of by-product



**Scheme 3.** Proposed mechanism of the oxygen activation for *m*-CPBA or *t*-BuOOH.



(benzaldehyde) was obtained (see Table 3, entry 2), implying that a greater contribution should come from the radical route (pathway c).

These contrasting mechanistic behaviors can be rationalized on the basis of the physical parameters of the substitutes on O–O bond in these two oxidants (*t*-BuOOH and *m*-CPBA). The chlorophenyl group of *m*-CPBA has a stronger ability to withdraw electron density from the peroxy unit alkyl group in *t*-BuOOH. This feature may result in an easy homolytic cleavage of the O–O bond (radical pathway) after the formation of a *t*-BuOO–Mn<sup>II</sup> fragment, while a heterolytic cleavage of the O–O bond is dominant in the *m*-CPBA case. This point can be confirmed by the rapid formation of high valent Mn species (e.g., O=Mn<sup>IV</sup> intermediate) when *m*-CPBA is used as oxidant (as suggested by the UV–vis results). Besides, the type of solvent should be another key factor in influencing the catalytic performance of **5**. In our case, aprotic solvent like CH<sub>3</sub>CN seems more suitable for the improvement of the catalytic performance of **5**.

#### 4. Conclusion

Hybrid manganese-based mesoporous material, prepared by covalent grafting of [Mn<sup>II</sup>(**1**)<sub>2</sub>](OAc)<sub>2</sub> (**3**) onto the surface of SBA-15, is an efficient heterogeneous catalyst for the epoxidation of alkenes (including terminal alkenes) with *m*-CPBA as the oxidant under mild conditions. The catalytic performance of this hybrid catalyst is solvent-dependent, relatively high catalytic activity and selectivity to epoxides could be obtained when an aprotic solvent (e.g., CH<sub>3</sub>CN) is present. UV–vis measurements of the reaction of oxidant in solution with homogeneous the [Mn<sup>II</sup>(**1**)<sub>2</sub>](OAc)<sub>2</sub> (**3**), revealed that high-valent Mn species, which are easily formed when CH<sub>3</sub>CN is used as the solvent, should be the main active intermediates for the epoxidation reaction with *m*-CPBA as the oxidant.

#### Acknowledgment

Financial support from the National Natural Science Foundation of China (20773050, 21173100) is gratefully acknowledged.

#### References

- [1] Z. Xi, N. Zhou, Y. Sun, K. Li, *Science* 292 (2001) 1139–1141.
- [2] G. Siene, R. Rieth, K.T. Rowbottom, *Ullmann's Encyclopedia of Industrial Chemistry*, 6th ed., Verlag Chemie, Weinheim, 2003, p. 269.
- [3] A. Ansmann, R. Kawa, M. Neuss, *Cosmetic composition containing hydroxyethers*, US Patent 7,083,780 B2, Aug. 1, 2006, To Cognis Deutschland, GmbH & Co. KG.
- [4] A.H. Hoveyda, *Chem. Rev.* 93 (1993) 1307–1370.
- [5] D. Swern (Ed.), *Organic Peroxides*, vol. 1, J. Wiley & Sons, Inc., 1970, p. 654.
- [6] W. Ye, R. Sangaiah, D.E. Degen, A. Gold, K. Jayaraj, K.M. Koshlap, G. Boysen, J. Williams, K.B. Tomer, V. Mocanu, N. Dicheva, C.E. Parker, R.M. Schaaper, L.M. Ball, *J. Am. Chem. Soc.* 131 (2009) 6114–6123.
- [7] S. Quideau, G. Lyvinec, M. Marguerit, K. Bathany, A. Ozanne-Beaudenon, T. Buffeteteau, D. Cavagnat, A. Chénéde, *Angew. Chem. Int. Ed.* 48 (2009) 4605–4609.
- [8] B. Meunier, *Chem. Rev.* 92 (1992) 1411–1456.
- [9] J.T. Groves, M.K. Stern, *J. Am. Chem. Soc.* 109 (1987) 3812–3814.
- [10] M. Palucki, P.J. Pospisil, W. Zhang, E.N. Jacobsen, *J. Am. Chem. Soc.* 116 (1994) 9333–9334.
- [11] E.M. McGarrigle, D.G. Gilheany, *Chem. Rev.* 105 (2005) 1565–1602.
- [12] K.P. Ho, W.L. Wong, K.M. Lam, C.P. Lai, T.H. Chan, K.Y. Wong, *Chem. Eur. J.* 14 (2008) 7988–7996.
- [13] S.H. Lee, L. Xu, B.K. Park, Y.V. Mironov, S.H. Kim, Y.J. Song, C. Kim, Y. Kim, S. Kim, *Chem. Eur. J.* 16 (2010) 4678–4685.
- [14] A. Murphy, A. Pace, T.D.P. Stack, *Org. Lett.* 6 (2004) 3119–3122.
- [15] A. Murphy, T.D.P. Stack, *J. Mol. Catal. A* 251 (2006) 78–88.
- [16] R.I. Kureshy, N.H. Khan, S.H.R. Abdi, I. Ahmad, S. Singh, R.V. Jasra, *J. Catal.* 221 (2004) 234–240.
- [17] R.I. Kureshy, I. Ahmad, N.H. Khan, S.H.R. Abdi, S. Singh, P.H. Pandia, R.V. Jasra, *J. Catal.* 235 (2005) 28–34.
- [18] R.I. Kureshy, I. Ahmad, N.H. Khan, S.H.R. Abdi, K. Pathak, R.V. Jasra, *J. Catal.* 238 (2006) 134–141.
- [19] N.J. Schoenfeldt, A.W. Korinda, J.M. Notestein, *Chem. Commun.* 46 (2010) 1640–1642.
- [20] F. Song, C. Wang, J.M. Falkowski, L. Ma, W. Lin, *J. Am. Chem. Soc.* 132 (2010) 15390–15398.
- [21] M. Moghadam, I. Mohammadpoor-Baltork, S. Tangestaninejad, V. Mirkhani, H. Kargar, N. Zeini-Isfahani, *Polyhedron* 28 (2009) 3816–3822.
- [22] S. Tangestaninejad, M. Moghadam, V. Mirkhani, I. Mohammadpoor-Baltork, M.S. Saeedi, *Appl. Catal. A: Gen.* 381 (2010) 233–241.
- [23] T.C.O. Mac Leod, V. Palaretti, V.P. Barros, A.L. Faria, T.A. Silva, M.D. Assis, *Appl. Catal. A: Gen.* 361 (2009) 152–159.
- [24] T.J. Terry, T.D.P. Stack, *J. Am. Chem. Soc.* 130 (2008) 4945–4953.
- [25] M. Jia, A. Seifert, W.R. Thiel, *Chem. Mater.* 15 (2003) 2174–2180.
- [26] M. Jia, A. Seifert, W.R. Thiel, *J. Catal.* 221 (2004) 319–324.
- [27] J. Tang, L. Wang, G. Liu, Y. Liu, Y. Hou, W. Zhang, M. Jia, W.R. Thiel, *J. Mol. Catal. A: Chem.* 313 (2009) 31–37.
- [28] W.R. Thiel, M. Angstl, T. Priermeier, *Chem. Ber.* 127 (1994) 2373–2379.
- [29] D. Zhao, Q. Huo, J. Feng, B.F. Chmelka, G.D. Stucky, *J. Am. Chem. Soc.* 120 (1998) 6024–6036.
- [30] H. Zhang, Y. Wang, L. Zhang, G. Gerritsen, H.C.L. Abbenhuis Rutger, A. van Santen, C. Li, *J. Catal.* 256 (2008) 226–236.
- [31] S. Gago, Y. Zhang, A.M. Santos, K. Köhler, F.E. Kühn, J.A. Fernandes, M. Pillinger, A.A. Valente, T.M. Santos, P.J.A. Ribeiro-Claro, I.S. Gonçalves, *Micropor. Mesopor. Mater.* 76 (2004) 131–136.
- [32] S.M. Bruno, J.A. Fernandes, L.S. Martins, I.S. Gonçalves, M. Pillinger, P. Ribeiro-Claro, J. Rocha, A.A. Valente, *Catal. Today* 114 (2006) 263–271.
- [33] S. Gago, J.A. Fernandes, J.P. Rainho, R.A. Sá Ferreira, M. Pillinger, A.A. Valente, T.M. Santos, L.D. Carlos, P.J.A. Ribeiro-Claro, I.S. Gonçalves, *Chem. Mater.* 17 (2005) 5077–5084.
- [34] A. Stein, M.H. Lim, *Chem. Mater.* 11 (1999) 3285–3295.
- [35] S. McCann, M. McCann, R.M.T. Casey, M. Jackman, M. Devereux, V. McKee, *Inorg. Chim. Acta* 279 (1998) 24–29.
- [36] H.H. Monfared, V. Aghapoor, M. Ghorbanloo, P. Mayer, *Appl. Catal. A: Gen.* 372 (2010) 209–216.
- [37] C. Hureau, G. Blondin, M. Charlot, C. Philouze, M. Nierlich, M. Césario, E. Anxolabéhère-Mallart, *Inorg. Chem.* 44 (2005) 3669–3683.
- [38] S. Groni, P. Dorlet, G. Blain, S. Bourcier, R. Guillot, E. Anxolabéhère-Mallart, *Inorg. Chem.* 47 (2008) 3166–3172.
- [39] T. Kurahashi, A. Kikuchi, Y. Shiro, M. Hada, H. Fujii, *Inorg. Chem.* 49 (2010) 6664–6672.
- [40] S. Romain, C. Duboc, F. Neese, E. Rivière, L.R. Hanton, A.G. Blackman, C. Philouze, J.-C. Leprêtre, A. Deronzier, M.-N. Collomb, *Chem. Eur. J.* 15 (2009) 980–988.
- [41] M. Hoogenraad, K. Ramkisoensing, W.L. Driessen, H. Kooijman, A.L. Spek, E. Bouwman, J.G. Haasnoot, J. Reedijk, *Inorg. Chim. Acta* 320 (2001) 117–126.
- [42] S. Biswas, K. Mitra, S.K. Chattopadhyay, B. Adhikary, *Transition Met. Chem.* 30 (2005) 393–398.
- [43] R. van Gorkum, J. Berding, D.M. Tooke, A.L. Spek, J. Reedijk, E. Bouwman, *J. Catal.* 252 (2007) 110–118.
- [44] R. Giovannetti, L. Alibabaei, F. Pucciarelli, *Inorg. Chim. Acta* 363 (2010) 1561–1567.
- [45] J.T. Groves, M.K. Stern, *J. Am. Chem. Soc.* 110 (1988) 8628–8638.
- [46] D. Feichtinger, D.A. Plattner, *Angew. Chem. Int. Ed. Engl.* 36 (1997) 1718–1719.
- [47] W. Adam, K.J. Roschmann, C.R. Saha-Möller, D. Seebach, *J. Am. Chem. Soc.* 124 (2002) 5068–5073.
- [48] K.P. Bryliakov, D.E. Babushkin, E.P. Talsi, *J. Mol. Catal. A: Chem.* 158 (2000) 19–35.